

Simulations of Sensing & Control for Advanced Virgo+ for O5

M. Boldrini^{1*}, D. Bersanetti², J. Casanueva Diaz³, C. De Rossi³,
M. Mantovani³, S. Melo³, M. Pinto³, P. Spinicelli³

¹INFN - Sezione di Roma, P.le Aldo Moro, 2, 00185 Roma (RM) - Italy

²INFN - Sezione di Genova, Via Dodecaneso, 33, 16146 Genova (GE) - Italy

³European Gravitational Observatory, Via Edoardo Amaldi, 5, 56021 Cascina (PI) - Italy

E-mail: mattia.boldrini@ego-gw.it

Abstract. The Phase II upgrade of Advanced Virgo+ phase I aims to increase the sensitivity of the interferometer to gravitational waves, both by reducing control noise below 10 Hz and making the interferometer more robust to thermal effects, which allows to increase the input power without degrading the detector performances. This upgrade radically modifies the optical layout, replacing the linear recycling cavities with longer, folded cavities that are geometrically stable but introduce four additional mirrors. These elements bring new degrees of freedom that interact in complex ways with the rest of the instrument, posing challenges for the control system. Optical simulations are essential for guiding the design and implementation of this upgrade. They help develop the sensing scheme, model the coupling between degrees of freedom, establish requirements, and identify critical challenges. We present the simulation groundwork to prepare the sensing and control scheme for Phase II.

1 Introduction

The current version of the Virgo interferometer, called Advanced Virgo+, included for the first time in this experiment a Signal Recycling cavity in its design. This upgrade, while effective in shaping the sensitivity curve of the interferometer, critically highlighted the well known design constraint of both recycling cavities being marginally stable. While the interferometer can, and indeed does, work in this configuration and it was able to join the O4 observation run, the complexity cost of this design constraint has become such that, for the next iteration of the experiment, the Virgo Collaboration has initiated a campaign to design and prepare the upgrade to stable recycling cavities. At the end of 2024, this campaign culminated in the selection of the baseline configuration of Advanced Virgo+ for O5.

The Interferometer Sensing & Control (ISC) team heavily contributed to this accomplishment through optical simulations. In this work we deliver an overview of our conclusions.



2 Baseline Configuration of Advanced Virgo+ for O5

The optical layout of Advanced Virgo+ for O5 is represented (simplified) in the following Fig. 1 [1].

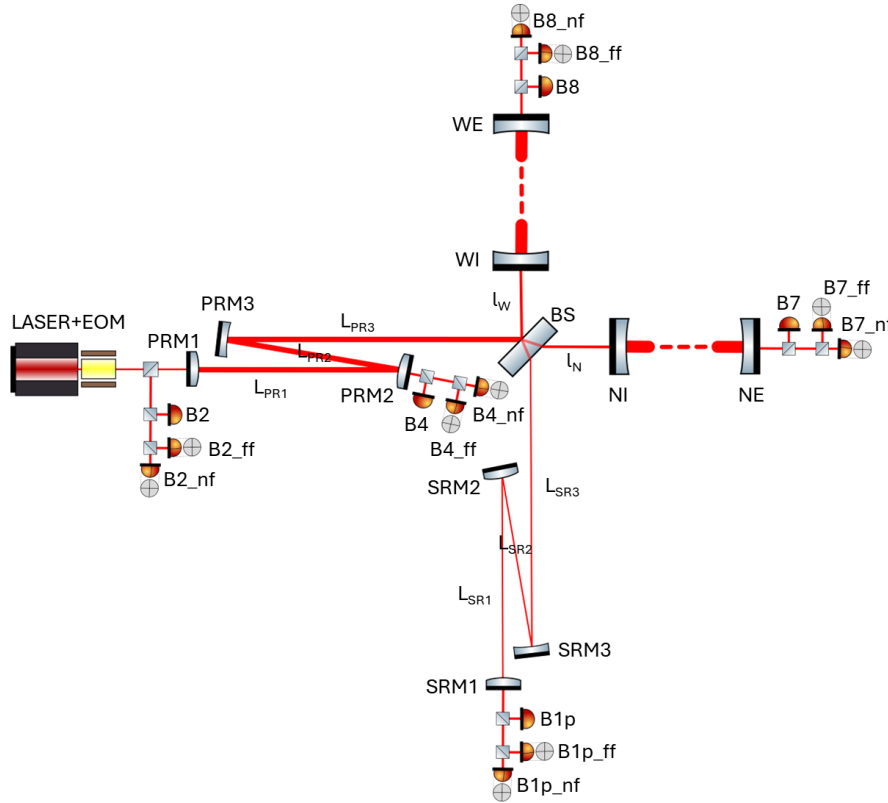


Figure 1: Simplified optical layout of Advanced Virgo+ for O5. The laser and *EOM* generate the carrier and sidebands injected into the interferometer. The *Power Recycling Mirrors* (PRM*) with *North Input/West Input* (NI/WI) form the *Power Recycling Cavity* (PRC), while the *Signal Recycling Mirrors* (SRM*) with NI/WI form the *Signal Recycling Cavity* (SRC). The arm Fabry–Perot cavities are defined by NI/WI with *North End/West End* (NE/WE) respectively. At the center is the *Beam Splitter* (BS). Distances between mirrors are labeled, as well as ports for longitudinal sensors (B*) and angular sensors (B*_nf/ff) in near- and far-field.

The design of the recycling cavities drives the choice of the control sidebands used to control the interferometer through PDH and Ward signals ([2], [3]), which in turn provides a figure of merit for the geometry itself. The baseline configuration was the result of this iterative process.

The error signals and the performances of the related loops are simulated using Finesse 3 [4].

The baseline design for the geometry of the recycling cavities is the following:

- **Power Recycling Cavity (PRC):** PRM1 → input mirrors, length = 35.2935 m, Gouy phase $\approx 26^\circ$;
- **Signal Recycling Cavity (SRC):** SRM1 → input mirrors, = 38.0083 m, Gouy phase $\approx 18^\circ$;

while the chosen control sidebands are:

- **SB1:** 6.37 MHz, resonant in the PRC;
- **SB2:** 27.61 MHz, resonant in both the PRC and the SRC;
- **SB3:** 78.57 MHz, resonant in the PRC, only 1-st order HG modes resonant in the SRC;
- **SB4:** 15.94 MHz, antiresonant in the PRC.

We now show the results of the simulation of the sensing for the baseline configuration.

3 Longitudinal Sensing

The longitudinal degrees of freedom of the baseline configuration are defined the same way as they were for Advanced Virgo+, accounting for the different design of the recycling cavities:

- PRCL (Power Recycling Cavity Length): $L_{PR1} + L_{PR2} + L_{PR3} + \frac{l_W + l_N}{2}$;
- SRCL (Signal Recycling Cavity Length): $L_{SR1} + L_{SR2} + L_{SR3} + \frac{l_W + l_N}{2}$;
- MICH: $\frac{l_W + l_N}{2}$;
- CARM: $\frac{L_W + L_N}{2}$;
- DARM: $\frac{L_W - L_N}{2}$.

We simulated a sweep of each of these degrees of freedom and their effect on every error signal available in the interferometer, that is every port B* shown in Fig. 1 demodulated at every sideband injected in the interferometer. The error signal associated with each degree of freedom is selected considering its optical gain (i.e. its slope across its zero), the width of its linear region and its ability to decouple different degrees of freedom. After this analysis, we build the longitudinal sensing matrix [1]. The most immediate figure of merit used to evaluate the sensing matrix is the decoupling angle α [5]:

$$\alpha = \arcsin |\det M_S| \quad (1)$$

where M_S is the sensing matrix, with each row normalized over its largest element. The perfect sensing matrix would look like a unity matrix ($\alpha = 90^\circ$), while the worst possible sensing matrix would have rows that are multiple of each other ($\alpha = 0^\circ$), for example because a degree of freedom dominates multiple signals and, after the normalization, the corresponding element on all of those rows is close to 1 and all the others are close to 0.

The simulated longitudinal sensing matrix that we obtain is reasonably well decoupled and can be made even better by implementing a hierarchical control. By setting up the unity gain frequencies of the longitudinal loops as per the following Tab. 1 we obtain a decoupling angle of $\alpha = 35.01^\circ$.

	CARM	DARM	PRCL	MICH	SRCL
signal	B4 SB1	B1 SB2	B2 SB1	B4 SB2 (I)	B4 SB2 (Q)
UGF	$\sim 7 \cdot 10^3$ Hz	70 Hz	40 Hz	15 Hz	4 Hz

Table 1: Expected *Unity Gain Frequency* UGFs of longitudinal loops for AdV+ for O5. We are considering an RF signal for DARM during the lock acquisition, in the steady state it will be handed off to B1 DC.

4 Angular Sensing

Advanced Virgo+ for O5 has 26 angular degrees of freedom:

- input beam tilt & shift;
- central interferometer: PRM1, PRM2, PRM3, BS, SRM1, SRM2, SRM3;
- arm cavities: DIFFp, DIFFm, COMMp, COMMm.

Each of them has a pitch (TX) and yaw (TY) component, although we consider them to be identical from the point of view of sensing and only simulate excitations of the yaw.

We expect the angular sensing to be considerably more complex than its longitudinal counterpart:

- The amount of degrees of freedom exceeds the availability of sensors: there will be degrees of freedom with no available quadrant to control them, but for some of them (PRM2 and SRM2, for example) the accuracy of local controls and/or centering loops based on cameras or dithering lines will be sufficient [6];
- Coupling among angular degrees of freedom is a well known issue: PRM*, BS and COMMp/m are usually competitors on the same signals, with the arms often dominating;

- The Signal Recycling cavity was particularly critical to align in the current iteration of Virgo: for the new design SB3 was specifically chosen to control this cavity by having *only* its first order modes resonating in it.

As expected, the coupling issues in the simulated sensing matrix are severe [1]: COMMp, COMMm and the BS dominate the signals for the PRC in such a way that we would need a combination of three signals to isolate the alignment of the PRC. This is an unfavourable situation: combining multiple signals piles up sensing noise and introduce more avenues of failure as it relies on the concurrent functioning of several QPDs at the same time.

To avoid this, we decided to change approach and exploit the presence of two quadrants at each port. These two sensors, separated by 90° of Gouy phase through appropriate telescopes, serve to deliver complete information about the wavefront of the impinging beam. We decided to use a combination of these two, for each degree of freedom, trading an increase of sensing noise of $\sqrt{2}$ across the board for better decoupling. The following Fig. 2 shows the idea behind this approach:

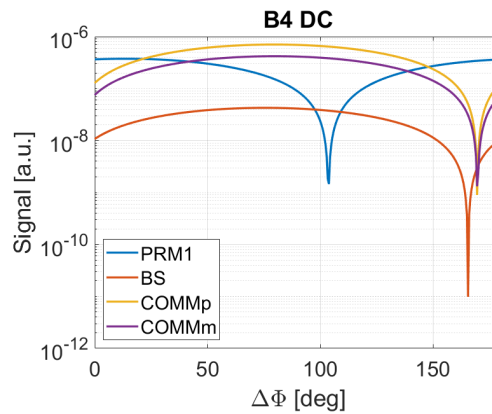


Figure 2: Simulated signals generated by B4_DC quadrants, rotated by $\Delta\Phi$, for misalignment of PRM1, BS, COMMp and COMMm. For $\Delta\Phi \approx 175^\circ$, the contribution of COMMp/m and BS on the signal is minimized.

Using this strategy, we are able to obtain a sensing matrix generally split in blocks [1] and with the following distribution of signals:

- PRM1: B4_DC, PRM2: X, PRM3: B4_SB4;
- BS: B1p_[SB2-SB1];
- SRM1: X, SRM2: X, SRM3: B1p_[SB3-SB2];
- DIFFp: B1p_SB2, DIFFm: B7±B8_DC, COMMp: B2_SB4, COMMm: B7±B8_[DC].

In this list, the “X” represents degrees of freedom without a dedicated quadrant, that will be aligned through other means (local controls, centering loops...), while we have kept the “best” signals in terms of optical gains for the most critical degrees of freedom, such as PRM3 and SRM3. Notice that the signal for SRM3 is built with combination of sidebands SB2 and SB3, using only the first order modes of SB3. The m modes for the arms are controlled through appropriate combinations of B7 and B8. Overall, the decoupling angle for this scheme is $\alpha = 9.15^\circ$.

5 Conclusions

The constraints that forced the choice of marginally stable cavities are still present, in particular the severely confined space to build them within the existing infrastructure. Producing a design of stable cavities that kept these constraints into account was a long and challenging effort that involved the vast majority of the Virgo Collaboration.

The Virgo ISC team provided valuable insight in this process by focusing on the controllability of the baseline configuration and concluded that this design is effectively controllable.

References

- [1] The Virgo Collaboration, “Advanced Virgo Plus for O5 – Technical Design Report”, 2025, <https://tds.virgo-gw.eu/?r=24767>
- [2] Drever, R.W.P., Hall, J.L., Kowalski, F.V., Hough, F.V., Ford, G.M., Munley, A.J. and Ward H., “Laser phase and frequency stabilization using an optical resonator”, *Applied Physics B*, vol. 31, pp. 97–105, 1983
- [3] Morrison, E., Meers, B.J., Robertson, D.I. and Ward, H., “Automatic alignment of optical interferometer”, *Applied Optics*, vol. 33, no. 22, pp. 5041–5049, 1994.
- [4] Brown, D.D., Freise, A., Cao, H.T., Ciobanu, A., Gobeil, J., Green, A., Hapke, P., Jones, P., van der Kolk, N., Kuns, K., Leavey, S., Perry, J.W., Rowlinson, S. and Sallé, M., (2025). FINESSE (3.0a32). Gitlab. <https://doi.org/10.5281/zenodo.12662017>
- [5] Mantovani, M. and Freise, A., 2008 *J. Phys.: Conf. Ser.* 122 012026
- [6] Boldrini, M., Mantovani, M., Bersanetti, D., Casanueva Diaz, J., De Rossi, C., “Simulations of the angular requirements for AdV+ phase II”, Virgo Technical Documentation System, VIR-0271A-25, The Virgo Collaboration, 2025, <https://tds.virgo-gw.eu/?r=24502>